NATIONAL ADVISORY COMMITTEE FOR AERONAUTICS

TECHNICAL NOTE 4071

A CORRELATION OF RESULTS OF A FLIGHT INVESTIGATION WITH RESULTS OF AN ANALYTICAL STUDY OF EFFECTS OF WING FLEXIBILITY ON WING STRAINS DUE TO GUSTS

By C. C. Shufflebarger, Chester B. Payne,
and George L. Cahen

Langley Aeronautical Laboratory
Langley Field, Va.

Washington
August 1957

NATIONAL ADVISORY COMMITTEE FOR AERONAUTICS

TECHNICAL NOTE 4071

A CORRELATION OF RESULTS OF A FLIGHT INVESTIGATION WITH RESULTS OF AN ANALYTICAL STUDY OF EFFECTS OF WING FLEXIBILITY ON WING STRAINS DUE TO GUSTS

By C. C. Shufflebarger, Chester B. Payne, and George L. Cahen

SUMMARY

An analytical study of the effects of wing flexibility on wing strains due to gusts has been made for four spanwise stations of a four-engine bomber airplane, and the results have been correlated with results of a previous flight investigation. The measured bending-strain amplification factors due to wing flexibility (ratio of strain for the flexible airplane to strain for the "rigid" airplane) at a station near the wing root were 1.09 when based on the ratio of root-mean-square values and approximately 1.19 when based on the ratio of strains obtained from distributions of strain peaks. The amplification factors decreased with each successive outboard station and then increased slightly at the tip station. When the airplane was considered to have three degrees of freedom (vertical motion and wing bending in the first and second symmetric bending modes), calculated amplification factors were in reasonable agreement with the measured results.

INTRODUCTION

The current trend toward thinner wings, higher speeds, and larger concentrations of mass in the wings has led to increased concern regarding the effects of wing flexibility on the aircraft structural loads in flight through atmospheric turbulence. A number of investigations have dealt with the development of analytical methods for calculating structural responses of airplanes to gusts (refs. 1 to 6). Also, a number of flight investigations of the effect of transient response associated with wing flexibility of present-day airplanes have been made by the National Advisory Committee for Aeronautics to determine the amplification of wing strain and accelerations induced by gusts (refs. 7 to 10), and correlations of these results with the results of analytical studies have been made.

In the initial studies the correlations of calculated and measured values were based primarily on the response of the airplane to simple and discrete gust disturbances and, although this approach has proven useful, it has not provided a clear description of the response of an airplane to continuous turbulence. The recent application of the method of generalized harmonic analysis to the problem of gust loads has, however, provided a technique that gives a more complete description of the response of an airplane to continuous turbulence. This approach has been applied in reference 1 in analytical studies, and the results obtained show good correlation with flight-test results evaluated on a "selected peak" basis for the overall effects of wing flexibility on the strains at the wing root stations of three airplanes.

In this paper the techniques of generalized harmonic analysis are applied in both the analytical calculations and in the analysis of the wing-strain measurements made on a four-engine bomber airplane during flight through rough air. (An evaluation of the data for the flight investigation on the basis of selected peaks is reported in ref. 10.) The use of generalized harmonic analysis techniques for both the calculated and measured values enables correlations to be made on the same basis and in more detail than in reference 1. Strain spectra, root-mean-square strain values, and the distribution of strain peaks were determined for each of four spanwise measuring stations, and the analytical methods of reference 1 are applied in order to calculate the same quantities. The method of reference 1 was extended to include the second symmetrical bending mode, in addition to the fundamental bending mode, as it appeared particularly pertinent for the outboard stations.

SYMBOLS USED IN BODY, TABLE, AND FIGURES

a	slope of lift curve of wing
b	span of wing
c	chord of wing
c_0	chord of wing at midsemispan
E	Young's modulus of elasticity
f	frequency, cps
g	acceleration due to gravity
I	bending moment of inertia

k statistical number of degrees of freedom

L scale of turbulence, ft

l distance from neutral axis to the extreme fiber

M_{c_0} moment of wing area about spanwise station under consideration, $\int_{y_j}^{b/2} c(y - y_j)\,dy$

$$M_{c_1} = \int_{y_j}^{b/2} c\omega_1(y - y_j)dy$$

$$M_{c_2} = \int_{y_j}^{b/2} c\omega_2(y - y_j)\,dy$$

$$M_{m_0} = \int_{y_j}^{b/2} m(y - y_j)\,dy$$

$$M_{m_1} = \int_{y_j}^{b/2} m\omega_1(y - y_j)\,dy$$

$$M_{m_2} = \int_{y_j}^{b/2} m\omega_2(y - y_j)dy$$

M_n generalized mass of nth mode

m mass per unit span of wing (except in eq. (4))

$N(y)$ number of strain peaks per second greater than a given strain level y

Δn incremental normal acceleration, g units

$$r_1 = \frac{2\int_0^{b/2} cw_1\,dy}{2\int_0^{b/2} c\,dy}$$

$$r_2 = \frac{2\int_0^{b/2} cw_1^2\,dy}{2\int_0^{b/2} c\,dy}$$

$$r_4 = \frac{2\int_0^{b/2} cw_2\,dy}{2\int_0^{b/2} c\,dy}$$

$$r_5 = \frac{2\int_0^{b/2} cw_1w_2\,dy}{2\int_0^{b/2} c\,dy}$$

$$r_6 = \frac{2\int_0^{b/2} cw_2^2\,dy}{2\int_0^{b/2} c\,dy}$$

S wing area

s distance traveled, $\frac{2V}{c_0}t$, half-chords

T arbitrary value of t, sec

T(f) amplitude of airplane frequency-response function

t time (zero at beginning of gust penetration)

V forward velocity of flight

W total weight of airplane

w_n deflection of elastic axis in nth mode, given in terms of unit tip deflection, positive upward

y distance along wing measured from airplane center line

$y(t)$ stationary random disturbance (strain amplitude)

ϵ strain

$$\lambda_1 = \frac{\omega_1 c_0}{2V}$$

$$\lambda_2 = \frac{\omega_2 c_0}{2V}$$

$$\mu_0 = \frac{8M_0}{a\rho c_0 s}$$

$$\mu_1 = \frac{8M_1}{a\rho c_0 s}$$

$$\mu_2 = \frac{8M_2}{a\rho c_0 s}$$

ρ mass density of air

σ root-mean-square value of output response

σ_U root-mean-square gust velocity

$\Phi_i( )$ input power-spectral-density function

$\Phi_o( )$ output power-spectral-density function

Ω frequency, radians/ft

ω_n natural circular frequency of vibration of nth mode

Primes denote derivatives with respect to s or σ.

Subscripts:

F	flexible case
j	spanwise station
n	natural modes of vibration
R	rigid case

APPARATUS, TESTS, AND ACCURACY OF MEASUREMENTS

The experimental data used in the present investigation were obtained from the flight investigation reported in reference 10. The airplane, flight conditions, and test procedures are described in detail in reference 10, and the description is partially repeated herein for completeness of this paper.

The characteristics of the test airplane are given in table I, and a three-view drawing of the test airplane is shown in figure 1. The estimated spanwise stiffness distribution is given in figure 2, and the estimated weight distribution for the test run considered herein is shown in figure 3.

The instrumentation used in this investigation consisted of electrical strain-gage bridges for measuring wing bending strains at the front and rear spars of wing stations 126, 255, 432, and 590, and an accelerometer mounted in each wing near the elastic axis at the estimated nodal point of the fundamental bending mode (station 278). All strain indications were recorded on a multichannel oscillograph. The outputs of the strain-gage installations at the inboard stations were recorded separately, whereas the gages on the front and rear spars of stations 432 and 590 were combined electrically to give a single output for each station. The natural frequency of the nodal-accelerometer recording system was approximately 9 cps. All recorders were correlated in time by means of an NACA 1/2-second chronometric timer.

The investigation was made at a speed of 250 mph for a weight of 105,900 pounds. In the course of the actual flight test, small variations from the specific test conditions occurred in the airspeed, altitude, and airplane weight. These variations were too small to be significant. A pull-up which was made at the same weight and speed was also analyzed for use in determining the equivalent "rigid" airplane strains.

The instrumentation, the character of the records, and the method of record reading were such that the overall accuracy of the individual measurements was estimated to be as follows:

Strain indications, percent	±5
Accelerations, g units	±0.05

The strain measurements in pull-ups and in laboratory load calibrations were linear within the accuracy of the measurements.

BASIS OF ANALYSIS

The object of the present study is to correlate data for analytically determined effects with data for experimentally determined effects of wing bending flexibility on the wing strains during flight through rough air. The overall effects of wing bending flexibility can be conveniently expressed in terms of amplification factors which are ratios of the strains for the flexible airplane to the strains for the rigid airplane condition. Two strain amplification factors are used in the analysis, one based on root-mean-square strains and the other on strains that a given number of peak strains equal or exceed.

The flexibility measures used involve comparison of actual incremental wing strains with the strains that would be obtained if the airplane were rigid. Since it is, of course, not possible to obtain the rigid-body reference strains in flight, some nearly equivalent strain must be used. The general practice, as in reference 1, has been to assume that the rigid-body strains are equal to the strains that would develop during pull-ups at accelerations equal to the accelerations that are measured at the nodal points during rough-air flights, and this practice has been followed herein. In utilizing the pull-up as the reference condition, the effects of quasi-static elastic twist and other aerodynamic features of the airplane are represented. The quasi-static elastic twist is, however, small for the test airplane and is neglected in this analysis. The acceleration values obtained from the nodal accelerometers in the left and right wings are averaged to give a single time history which is used as the rigid-body acceleration in rough air. The use of the average of the two nodal accelerometers largely eliminates the effects of roll and of unsymmetrical vibrations on the measured accelerations.

Inasmuch as the evaluation of the results of the flight investigation and the associated analytical results are based on the techniques of generalized harmonic analysis, a few basic concepts and relations that are needed are given here. One of the more important and useful characteristics of a stationary random disturbance is its power-spectral-density function. If $y(t)$ is a stationary random disturbance, the

power-spectral-density function or power spectrum of $y(t)$ is defined by

$$\Phi(f) = \lim_{T\to\infty} \frac{1}{T}\left| \int_{-T}^{T} y(t)\, e^{-2\pi i f t} dt \right|^2 \qquad (1)$$

where the bars designate the modulus of the complex quantity and T is an arbitrary value of t in seconds. The power spectrum $\Phi(f)$ can essentially be considered to describe the contributions of the various frequencies to the total power or mean-square value of the disturbance.

The power spectrum of a disturbance and the power spectrum of the response of the airplane to the disturbance are, for a linear system, related simply by

$$\Phi_o(f) = \Phi_i(f)\left| T(f) \right|^2 \qquad (2)$$

where $\Phi_i(f)$ is the power spectrum of the input, $\Phi_o(f)$ is the power spectrum of the output response, and $|T(f)|$ is the amplitude of the system frequency-response function which, in the present application, is the amplitude of the airplane wing bending-strain response to a unit sinusoidal gust disturbance of frequency f. In a subsequent section of this paper, the frequency-response functions $T(f)$ are determined analytically and applied in equation (2) in order to determine the expected strain spectra for comparison with the measured results.

The spectrum of the output response permits the determination of the mean square of the response and other statistical characteristics of the disturbance that are of interest. The root-mean-square value provides a simple and direct measure of the overall response intensity. Also, as in reference 1, the spectra for a Gaussian random process may be used to derive the average number of peaks per second $N(y)$ that exceed a given strain level y. The expression for obtaining the average number of peaks per second exceeding given values, as given in reference 1, is

$$N(y) = \left[\frac{\int_0^\infty f^2 \Phi_o(f)\, df}{\int_0^\infty \Phi_o(f)\, df} \right]^{1/2} e^{-y^2/2\sigma^2} \qquad (3)$$

where

$N(y)$ number of strain peaks per second greater than y

y strain amplitude

σ^2 mean-square value of the strain response, $\int_0^\infty \Phi_o(f)\,df$

Thus, equation (3) may also be written as

$$N(y) = \frac{\sigma_1}{\sigma} e^{-y^2/2\sigma^2}$$

where

$$\sigma_1^2 = \int_0^\infty f^2 \Phi_o(f)\,df$$

RESULTS

Experimental

Time histories of strain indications and nodal-point accelerations for a portion of a gust record and a pull-up are shown in figure 4. A preliminary check of the strain indications for the front and rear spars of stations 126 and 255 indicated that the strains in rough air relative to the strains in pull-ups were essentially the same for the front and rear spars at these stations and, therefore, only the front-spar strains were used to represent these stations.

Power spectra.- Power-spectral-density functions for the wing bending strains and rigid-body accelerations were computed from the time-history data for a 2-minute section of records by Tukey's calculation procedure for spectra estimation as presented in references 11 and 12. In determining the strain spectra from the measurements, the nature of the records made impractical the reading of the records at time intervals of less than 0.1 second; therefore, the range of the spectra was limited to 5 cps. The nodal-acceleration records, however, were read at intervals of 0.05 second; thus the spectra for the rigid condition covered the frequency range from 0 to 10 cps. Forty estimates of the power, equally spaced over the frequency range from 0 to 5 cps, were obtained for the

strain histories, and 20 estimates (due to a difference in reading intervals) were obtained for the rigid-body acceleration.

Since the wing strains in a pull-up are different at the various wing stations (fig. 4) the spectra of rigid-body strains also differ from station to station. To permit direct comparison between amplification effects at the various stations, the time histories of wing bending strain ϵ_j in rough air were normalized in the following manner:

$$\text{Normalized } \epsilon_j = \epsilon_j \frac{(\epsilon/g) \text{ at station 126 in a pull-up}}{(\epsilon_j/g) \text{ in a pull-up}}$$

The rigid-body acceleration history was also converted to a normalized rigid-body strain by multiplying by the strain per g at station 126 in a pull-up. This normalization permits direct comparison of all strain spectra with a single rigid-body strain spectrum. The normalized strain spectra obtained in the foregoing manner are shown in figure 5 for the frequency range from 0 to 5 cps. Because of the normalization the actual numerical values have no real significance, except at station 126, and do not reflect the actual strain variations between the different stations.

Peak counts.- A direct count of the strain peaks for all cases was not considered practical; therefore, the number of strain peaks per mile greater than a given strain level was estimated from the measured spectra of figure 5 by means of equation (3). The results are plotted in figure 6 as a function of strain level for the flexible and rigid cases at station 126.

In the evaluation of the integrals in equation (3), the spectra of figure 5 were used. Inasmuch as these spectra cover only the frequency range of 0 to 5 cps, the integrals could be determined only for this region. This approximation does not affect the reliability of the root-mean-square values, inasmuch as the numerical procedures used result in no loss of power but only in a distortion of the true spectrum; the power at frequencies above 5 cps appears as power at lower frequencies. The number of peaks exceeding given values is somewhat underestimated, however, as a result of this approximation, as is indicated in a subsequent section.

Amplification factors.- The magnitude of the flexibility effects can be shown by strain ratios, that is, the ratio of a measure of the strain for the flexible case to the comparable measure of strain for a reference rigid case. Inasmuch as the root-mean-square strains provide a simple measure of the strain levels, the ratios of the root-mean-square values for the flexible case to the corresponding values for the rigid

case give one measure of the strain amplification factor (obtained from the root-mean-square values given in fig. 5) and are plotted as a function of wing station in figure 7(a).

Another measure of the strain amplification due to flexibility that is frequently of interest is the ratio of the strain for the flexible airplane to the strain for the rigid airplane that has the same frequency of occurrence. This ratio may be more significant for fatigue studies than the ratio of the root-mean-square values and is determined as illustrated in figure 6 from the distributions of strain peaks for the flexible and rigid airplanes. Figure 6 shows that the ratio of the strain for the flexible airplane to the strain for the rigid airplane that has the same frequency of occurrence varies with strain level; the ratio is highest at the low strain values and, as can be shown analytically, approaches the ratio of the root-mean-square values at the higher strain levels. As in reference 1, the frequency of occurrence selected for determining the strain ratios was the frequency for the flexible airplane at a strain equal to twice the root-mean-square strain for the flexible airplane. This strain ratio for each of the four measuring stations is shown in figure 7(b).

Statistical reliability.- The statistical reliability of the power spectra determined from the 2-minute section of record was determined by the method of reference 11. The reliability of each power estimate for relatively flat spectra is expressed in terms of the statistical number of degrees of freedom k, where

$$k = \frac{n - \frac{m}{5}}{\frac{m}{2}} = \frac{1200 - \frac{40}{5}}{\frac{40}{2}} = 59.6 \qquad (4)$$

and

m number of uniformly spaced points over frequency range for which power estimates are obtained

n number of equally spaced observations taken over the length of the time history, $T/\Delta t$

For this value of k, figure 2 of reference 11 shows each individual power estimate to have 95-percent confidence limits from 0.68 to 1.35 of the value measured. Small peaks in the measured spectra may, therefore, be merely statistical fluctuations. The statistical reliability of the root-mean-square value, which is based on the integrated power, is considerably higher and is estimated to be reliable to within approximately ±10 percent.

Analytical

The results obtained in the analytical phase of this investigation were based on the relation of the random input disturbance (for a uniform spanwise gust), the output response of the airplane, and the frequency-response characteristics of the airplane as given in equation (2). Selection of a suitable input disturbance, calculation of the airplane frequency-response function, and determination of the output response by means of equation (2) was required. Inspection of the wing strain indications, as in figure 4, revealed that the second bending mode of vibration was of some importance at the outboard wing stations; the method of reference 1 was therefore extended to include the second symmetrical bending mode. The determination of the input gust disturbance, the airplane frequency-response or transfer functions, and the output responses are discussed in the following sections.

Input disturbance.- Recent theoretical studies, such as reference 13, have used the following expression to approximate the spectrum of vertical gust velocity:

$$\Phi_i(\Omega) = \sigma_U^2 \frac{L}{\pi} \frac{1 + 3\Omega^2 L^2}{(1 + \Omega^2 L^2)^2} \tag{5}$$

where

σ_U^2 mean-square gust velocity, $(\text{ft/sec})^2$

L scale of turbulence, ft

Ω frequency, $2\pi/\lambda$ (where λ is gust wave length in feet), radians/ft

For present purposes it is convenient to express the gust spectrum in terms of the frequency argument f in cycles per second, where

$$f = \frac{V}{2\pi} \Omega$$

and V = 368 ft/sec. In terms of this frequency argument, the gust power spectrum is given by

$$\hat{\Phi}_i(f) = \Phi_i(\Omega) \frac{d\Omega}{df}$$

$$= \sigma_U^2 \frac{2L}{V} \frac{1 + 3\left(\frac{2\pi Lf}{V}\right)^2}{\left[1 + \left(\frac{2\pi Lf}{V}\right)^2\right]^2}$$

Representative values of L for atmospheric turbulence are believed to vary from several hundred feet to more than 1,000 feet. The spectra for values of L of 400, 1,000 and 2,000 feet are shown in figure 8 for a value of σ_U^2 of 1. The value of L equal to 1,000 feet was selected for the present analysis as being of the correct order, on the basis of measured data (ref. 12), although calculations were also made for other values of L.

Frequency-response functions.- The frequency-response characteristics were obtained for the airplane bending-strain response to continuous sinusoidal gust encounters on the basis of the method of reference 1. In addition to calculations for the rigid condition, the frequency-response functions were calculated for two separate flexible conditions: (1) the airplane with two degrees of freedom (as in ref. 1), vertical motion and wing bending in the fundamental mode, and (2) the airplane with three degrees of freedom, vertical motion and wing bending in the fundamental mode and second mode (first and second symmetrical bending modes).

Although airplane pitch may be important in the response of an airplane to gusts, pitch response was not included in the calculations because of increased complexity. The equations necessary for including the second symmetrical mode are derived in the appendix, and the airplane loading, physical constants, and basic parameters are given in table I. The slope of the lift curve a was estimated to be 5.00 per radian for the test airplane, and this value was used as being more appropriate in the calculations than the value of 6.28 used in reference 1. In using the method of reference 1 to obtain the amplitude of the airplane bending response, the results were obtained in terms of a bending-moment coefficient per foot per second. The equations necessary for converting the bending-moment coefficients to strains are given in the appendix of the present report. The frequency-response functions obtained for the wing stations at which flight measurements were made are shown in figure 9.

Output response.- Output-response spectra were obtained for each wing station by using in equation (1) the calculated frequency-response functions and the assumed input spectrum of equation (5) for $\sigma_U^2 = 1$. The output spectra were calculated for a frequency range of 0 to 10 cps in order to include the effect of the second symmetrical mode that peaks at approximately 7 cps. For convenience in making comparisons, the calculated output spectra for the rigid airplane and the flexible airplane (three degrees of freedom) for the wing stations at which the flight measurements were made and a value of L of 1,000 feet were normalized in the manner used in obtaining figure 5 (so that direct comparisons could be made) and are shown in figure 10. The results for frequencies of only 0 to 5 cps are shown in this figure because of the very low values at the higher frequencies. In order to show the results for the higher

frequencies, and in particular to indicate the effect of the second bending mode, the complete frequency-response functions for frequencies of 0 to 10 cps are shown in figure 11 with a logarithmic ordinate scale.

Amplification factors.- The amplification factors or strain ratios based on the ratio of the root-mean-square strain for the flexible airplane to that for the rigid airplane were obtained from spectra such as those in figure 10 (square root of area under spectra). These calculated values for both two degrees and three degrees of freedom are shown in figure 12(a), plotted as a function of wing station for a value of L of 1,000 feet, along with the measured values from figure 7(a).

The number of strain peaks per mile greater than given strain levels were obtained for each wing station by use of equation (3) in order to determine amplification factors or strain ratios based on the distribution of peak strain values, as was done for the experimental results shown in figure 6. The calculated values for both two degrees and three degrees of freedom are shown in figure 12(b) for a value of L of 1,000 feet, along with the measured values from figure 7(b).

DISCUSSION

Experimental Results

Power spectra.- Inspection of the spectra of wing strains in flight through turbulence (fig. 5) reveals two features of interest. In the frequency range below approximately 0.5 cps, an amplification of wing strains that increases roughly in proportion to the distance from the center line is apparent. It is felt that this increase is primarily due to factors such as spanwise gust variations and airplane rolling motions rather than wing flexibility. At the fundamental bending-mode frequency of 2.7 cps, the effects of wing flexibility are evidenced by the bump that appears in the spectra. The spectra indicate that flexibility effects near the fundamental bending-mode frequency are greatest at the most inboard station and least at the two outboard stations.

The effects of the second symmetrical bending mode are not evident in the measured spectra, inasmuch as the frequency of the second bending mode is about 7 cps and the spectra in figure 5 are shown to only 5 cps. Because of the method of obtaining the spectra, however, the power at higher frequencies is not lost but is reflected and appears as power at frequencies of less than 5 cps; in particular, the power associated with the second symmetric mode at approximately 7 cps may be expected to appear at 3 cps. This characteristic of reflection of the power above the highest resolved frequency (5 cps in the present case) has been termed "aliasing" (ref. 12). The measured spectra are distorted to the extent

of this reflection. The power expected at the higher frequencies is small, however, as indicated by inspection of the strain records, and the distortion expected is also small.

The measured spectra also show a slight tendency to increase in power at frequencies above approximately 3.5 cps. This tendency may be a reflection of the first antisymmetrical mode, believed to be at about 5 cps, as indicated in reference 10.

Amplification factors.- The ratios of the measured values of root-mean-square strain for the flexible airplane to those for the rigid airplane (fig. 7(a)) indicate that an amplification factor of approximately 1.1 applies for all wing stations. However, part of the amplification (especially at the outboard stations) is due to differences in the spectra of figure 5 at frequencies below approximately 0.5 cps that, as previously noted, are felt to result from factors such as spanwise gust variations and rolling motions rather than from wing flexibility. In order to obtain amplification factors that, insofar as possible, reflect only the amplification due to flexibility, the spectra for the flexible condition in figure 5 were reduced to the same values as the spectrum for the rigid condition in the frequency range from 0 to 0.5 cps on the assumption that these differences between the spectra were not due to flexibility. The amplification factors obtained from these adjusted spectra are also shown in figure 7(a) and indicate that the amplification factor due to flexibility decreased from a value of 1.09 at station 126 to a value of 1.03 at station 432 and then increased to a value of 1.05 at station 590.

Amplification factors based on distributions of strain peaks as in figure 6 are shown in figure 7(b) for both the measured and adjusted spectra of figure 5. These amplification factors are, in general, considerably higher than those based on root-mean-square values but indicate the same trend of flexibility effects; that is, the amplification factor based on the adjusted spectra of figure 5 decreased from a value of 1.19 at station 126 to a value of 1.03 at station 432, and then increased to a value of 1.11 at station 590. The amplification factors based on the measured spectra are greater than those based on the adjusted spectra by an increment of 0.02 to 0.07. All the amplification factors in figure 7(b) determined from the spectra of figure 5 and by the use of equation (3) are believed to be somewhat too low because they are based on spectrum measurements which cover only the frequency range from 0 to 5 cps. A few checks of these ratios were made by actual counts of strain peaks and they yielded values that were greater by an increment of about 0.05 than those obtained from the spectra and the use of equation (3). It would thus appear that amplification effects due to flexibility, as obtained from the measured spectra, may be underestimated by this amount in figure 7(b).

The preceding discussion indicates that both the amplification factors used - the ratio of root-mean-square values and the factor determined from distributions of strain peaks - show the largest effects of flexibility at the most inboard station and the smallest at station 432. It is also of interest to note that increasing the amplification factors obtained from distributions of strain peaks (fig. 7) by an increment of 0.05 (the approximate amount by which the strain peaks are believed to be underestimated) results in substantial agreement between the results from the spectra of figure 5 and the amplification factors obtained in reference 10 on a basis of selected peaks.

Comparison of Calculated and Experimental Results

Frequency-response functions.- Inspection of the calculated frequency-response functions in figure 9 indicates that the amplification of a wing bending strain due to fundamental bending-mode response at approximately 2.5 cps is largest at the inboard wing stations while the amplification of a wing bending strain due to second bending-mode response at approximately 6.5 cps is largest at the outboard stations. The calculated frequency-response functions for two degrees and three degrees of freedom in figure 9 are approximately the same for frequencies below about 4 cps. When the rapid decrease of input power with frequency is considered (fig. 8), it is evident that the output power will be little changed by the effect of the second bending mode. The differences in the frequency-response functions at frequencies above 4 cps, however, will result in a larger number of peak strains above a given value because of the fact that the number of peaks depends more heavily on the higher frequencies of the spectrum (eq. (3)).

Power spectra.- Direct comparison of the output spectra of figures 5 and 10 on the basis of the ordinate values is not justified because the intensity of the input for the measured spectra is not known and because a value of 1 was used for σ_U^2 in the calculations. The calculated output spectra of figure 10 for a value of L of 1,000 feet, however, resemble the measured spectra of figure 5 except for the differences in the frequency range below approximately 0.5 cps which, as previously noted, are believed to be due to factors not related to wing flexibility. Both the measured and calculated spectra show a large peak power due to rigid-body motions at a frequency below 1.0 cps and a secondary small peak (indicating response of first bending mode) around 2.5 cps, with the secondary peak decreasing in both cases as the stations become more outboard. The measured spectra, however, show greater power in the secondary peak relative to that in the primary peak than do the calculated spectra. The reason for this discrepancy is not clear, but the effects of pitching motions on the measured spectra at low frequencies and the use of an assumed turbulence spectrum in the calculations may

account for at least a part of the discrepancy. In addition, there is a greater decrease in power of the secondary peak, as the stations become more outboard, for the calculated spectra than for the measured spectra, and part of this decrease (although possibly only a small part) is a reflection (due to the aliasing effect) of the power associated with the second symmetrical bending mode at about 7 cps (see outboard stations, fig. 4). It should be noted that although the calculated spectra shown in figure 10 are for the three-degree-of-freedom case (two structural modes), the spectra are essentially the same as for the two-degree-of-freedom case (see transfer functions in fig. 9) for frequencies below 4.0 cps.

The calculated and measured spectra of figures 5 and 10 cannot be compared directly to determine the effects of the second symmetrical mode in bending on the strains, since the measurements covered only the frequency range from 0 to 5 cps. An indication of the very low power due to this mode is shown in the plot of the calculated spectra for the three-degree-of-freedom condition on a logarithmic scale in figure 11, where the peak power of the spectra is approximately one thousand times as great as the peak power at 6 cps for the outboard wing stations.

Amplification factors.- Comparisons of the adjusted and calculated effects of flexibility in figure 12(a), based on the ratio of root-mean-square values of the adjusted spectra of figure 5 and the results for both two and three degrees of freedom for a value of L of 1,000 feet, indicate that the adjusted values of amplification factors are in substantial agreement with the calculated values except at the most outboard station where the value is 1.05 compared with the calculated value of approximately 1.02. The calculated factors shown in figure 12(a) decrease from a value of 1.12 at the center line to a value of 1.02 at 0.6 of the semispan from the center line, and the value is about 1.02 or less for stations outboard of this point. Measurements and calculations therefore agree and show the largest effects of flexibility at the most inboard stations, but a discrepancy between the calculated and adjusted results is apparent at the most outboard stations.

Comparison of the effects of flexibility (fig. 12(b)) on the basis of amplification factors determined from distributions of peak strains, as in figure 6, indicates that in general the calculated results for the three-degree-of-freedom condition and a value of L of 1,000 feet are in relatively good agreement with the results derived from the adjusted spectra of figure 5 (shown in fig. 7(b)) except at the most outboard stations. The calculated amplification factors shown in figure 12(b) decrease from a value of 1.29 at the center line to a value of 1.04 at 0.5 of the semispan from the center line, increase to a value of 1.07 at 0.8 of the semispan, and then decrease. The calculated amplification factors for the two- and three-degree-of-freedom conditions (fig. 12(b)) are in substantial agreement at the inboard stations, but the results

for two degrees of freedom show much lower amplification factors at the outboard stations and indicate that the second symmetric bending mode has a large effect on the amplification factors at these stations. The higher amplification factors for the calculated results at the two outboard stations when the second symmetric bending mode is taken into account are, as previously mentioned, the result of differences in the spectra at the higher frequencies that have small effects on the root-mean-square values.

The effect of the choice of gust input, slope of the lift curve, and frequency range on the calculated amplification factors is of interest. A lower value of L in equation (5) will result in a higher amplification factor; for example, the use of a value of L of 400 feet yields an amplification factor based on root-mean-square values of approximately 1.16 for station 126, compared with approximately 1.10 for a value of L of 1,000 feet. A higher lift-curve slope reduces the amplification factor, and for these calculations the use of a lift-curve slope of 6.28 instead of 5.00 would have approximately the same effect as the use of a value of L of 1,000 feet instead of 400 feet. The calculated amplification factors obtained from distributions of strain peaks are dependent on the upper limit of integration used in equation (3) because it is not practical to integrate to infinity, and the effect of a change in the upper limit on the amplification factor depends upon the frequency-response functions. In the present case, however, both analytic considerations and the recorded data place the upper limit of the integration at about 10 cps.

In assessing the reliability of the analytic calculations it was noted that although the measured and calculated results are in relatively good agreement, some discrepancies are present. Inaccuracies in the calculations can, of course, arise from a large number of sources and will require further study. In the present case an assumed gust input was used, and the effect of factors such as airplane pitching motions, spanwise gust effects, and the antisymmetric bending mode were neglected. Although uncertainties in the calculations may arise from the factors mentioned, the present results indicate that the methods used provide reasonable first-order estimates of the magnitude and character of the effects of flexibility on the bending strains at the various spanwise stations for unswept-wing airplanes.

CONCLUSIONS

The effects of wing flexibility on the wing strains that result from gust encounter have been examined on a power-spectral basis. Both flight results and analytical results have been considered for a four-engine bomber airplane, and correlations between the measured and analytical results have been made. The effects of wing flexibility on the wing

strains were measured in terms of amplification factors based on the ratio of the strain for the flexible condition to the strain for the "rigid" condition, and results were obtained for four spanwise stations of the wing. The effect of including the second symmetric bending mode in addition to the fundamental bending mode in the calculations was also evaluated. The study led to the following results:

1. Comparison of the measured strain spectra for the flexible and rigid conditions showed strain amplifications in the frequency range below 0.5 cps, especially at the outboard wing stations, that are attributed to the effect of factors such as spanwise gust variations and airplane rolling motions rather than to flexibility effects.

2. The measured strain amplification factors due to wing flexibility at a station near the wing root were 1.09, on the basis of the ratio of root-mean-square strains, and approximately 1.19 on the basis of the ratio of strains derived from distributions of strain peaks. The amplification factors decreased with each successive outboard station and then increased slightly at the most outboard measuring station.

3. The calculated output spectra were in reasonable agreement with the measured spectra except at low frequencies, where the differences are attributed to extraneous factors. At the outboard stations it was necessary to include the effect of the second symmetric bending mode in the calculations in order to estimate adequately the effect of flexibility on the distributions of strain peaks.

4. Both calculations and measurements indicated that the second symmetric bending mode had a very small effect on the root-mean-square strains but that, for strain amplification factors determined from distributions of strain peaks, the second symmetric bending mode had a pronounced effect at the outboard wing stations.

5. Although uncertainties in the calculations may arise from a number of factors, the present results indicate that calculations based on power-spectral techniques may provide reliable estimates of the magnitude and character of wing flexibility effects on wing strains in gusts for unswept-wing airplanes.

Langley Aeronautical Laboratory,
National Advisory Committee for Aeronautics,
Langley Field, Va., May 27, 1957.

APPENDIX

DERIVATION OF THE FREQUENCY-RESPONSE FUNCTIONS INCLUDING VERTICAL MOTION AND FIRST AND SECOND SYMMETRICAL MODES OF WING BENDING

In order to include the effects of a higher mode in the analytical results of this paper, the gust-response analysis of reference 1 was extended to include the second symmetrical wing bending mode. Addition of the second symmetrical wing bending mode simply adds a term to each of the response equations of reference 1, and an additional equation is obtained for the second mode. This appendix shows the effect of the additional mode on the pertinent equations but does not attempt to present the complete derivation, which should be self-evident.

Symbols Used in Appendix

a	slope of lift curve of wing
a_n	deflection coefficient for nth mode, function of time alone
b	span of wing
c	chord of wing
c_0	chord of wing at midsemispan
E	Young's modulus of elasticity
I	bending moment of inertia
K_j	nondimensional bending-moment factor, $\frac{M_j}{\frac{a}{2}\rho U V M c_0}$
k	reduced-frequency parameter, $\frac{\omega c_0}{2V}$
l	distance from neutral axis to extreme fiber

M_{c_0} moment of wing area about spanwise station under consideration, $\int_{y_j}^{b/2} c(y - y_j)\,dy$

$$M_{c_1} = \int_{y_j}^{b/2} c\omega_1(y - y_j)\,dy$$

$$M_{c_2} = \int_{y_j}^{b/2} c\omega_2(y - y_j)\,dy$$

M_j net incremental bending moment at wing station j, $K_j \frac{a}{2} \rho U V M_{c_0}$

$$M_{m_0} = \int_{y_j}^{b/2} m(y - y_j)\,dy$$

$$M_{m_1} = \int_{y_j}^{b/2} m\omega_1(y - y_j)\,dy$$

$$M_{m_2} = \int_{y_j}^{b/2} m\omega_2(y - y_j)\,dy$$

M_n generalized mass of nth mode

m mass per unit span of wing

$$r_1 = \frac{2\int_0^{b/2} cw_1\,dy}{2\int_0^{b/2} c\,dy}$$

$$r_2 = \frac{2\int_0^{b/2} cw_1^2\,dy}{2\int_0^{b/2} c\,dy}$$

$$r_4 = \frac{2\int_0^{b/2} cw_2\,dy}{2\int_0^{b/2} c\,dy}$$

$$r_5 = \frac{2\int_0^{b/2} cw_1w_2\,dy}{2\int_0^{b/2} c\,dy}$$

$$r_6 = \frac{2\int_0^{b/2} cw_2^2\,dy}{2\int_0^{b/2} c\,dy}$$

s,σ distance traveled, $\frac{2V}{c_0}t$, half-chords

$T(f)$ amplitude of airplane frequency-response function

t time (zero at beginning of gust penetration)

U gust velocity

u vertical velocity of gust

V forward velocity of flight

w_n deflection of elastic axis in nth mode, given in terms of unit tip deflection, positive upward

y distance along wing measured from airplane center line

z_n response coefficient based on a_n, $\frac{V}{Uc_0} a_n$

ϵ strain, normal

$\lambda_1 = \frac{\omega_1 c_0}{2V}$

$\lambda_2 = \frac{\omega_2 c_0}{2V}$

$\mu_0 = \frac{8M_0}{a\rho c_0 s}$

$\mu_1 = \frac{8M_1}{a\rho c_0 s}$

$\mu_2 = \frac{8M_2}{a\rho c_0 s}$

ρ mass density of air

$1 - \varphi$ function which denotes growth of lift on an airfoil following a sudden change in angle of attack (Wagner function)

ψ function which denotes growth of lift on rigid wing entering a sharp-edge gust (Küssner function)

ω_n natural circular frequency of vibration of nth mode

Subscripts:

j spanwise station

n natural modes of vibration

By following the procedure used in reference 1 for obtaining the response equations (eqs. (16) and (17) of ref. 1) for only two degrees of freedom, vertical motion and wing fundamental bending, the following response equations are obtained for the addition of the second symmetrical mode:

$$\mu_0 z_0'' = -2\int_0^s \left(z_0'' + r_1 z_1'' + r_4 z_2''\right)\left[1 - \varphi(s-\sigma)\right] d\sigma + \int_0^s \frac{u'}{U} \psi(s-\sigma) d\sigma \tag{A1}$$

$$\mu_1 z_1'' + \mu_1 \lambda_1^2 z_1 = -2\int_0^s \left(r_1 z_0'' + r_2 z_1'' + r_5 z_2''\right)\left[1 - \varphi(s-\sigma)\right]d\sigma +$$

$$r_1 \int_0^s \frac{u'}{U}\,\psi(s-\sigma)d\sigma \tag{A2}$$

$$\mu_2 z_2'' + \mu_2 \lambda_2^2 z_2 = -2\int_0^s \left(r_4 z_0'' + r_5 z_1'' + r_6 z_2''\right)\left[1 - \varphi(s-\sigma)\right]d\sigma +$$

$$r_4 \int_0^s \frac{u'}{U}\,\psi(s-\sigma)d\sigma \tag{A3}$$

The equation that defines a bending-moment factor K_j at wing station y_j (from eq. (22) of ref. 1) takes the following form:

$$K_j = \frac{-8M_{m_0}}{a\rho c_0 M_{c_0}}\left(z_0'' + \frac{M_{m_1}}{M_{m_0}} z_1'' + \frac{M_{m_2}}{M_{m_0}} z_2''\right) - 2\int_0^s \left(z_0'' + \frac{M_{c_1}}{M_{c_0}} z_1'' + \right.$$

$$\left.\frac{M_{c_2}}{M_{c_0}} z_2''\right)\left[1 - \varphi(s-\sigma)\right]d\sigma + \int_0^s \frac{u'}{U}\,\psi(s-\sigma)d\sigma \tag{A4}$$

In order to reduce the response equations (A1) to (A4) to the special case of sinusoidal gust encounter where the gust has a frequency ω, the quantities u, z_0, and z_1 may all be taken proportional to e^{iks}, where $k = \frac{\omega c_0}{2V}$, as shown in reference 1. By following the procedure used in reference 1, equations (A1) to (A4) are reduced to the following form:

$$-\mu_0 k^2 z_0 = -2ik\left(z_0 + r_1 z_1 + r_4 z_2\right)(F + iG) + (P + iQ) \tag{A5}$$

$$-\mu_1 k^2 z_1 + \mu_1 \lambda_1^2 z_1 = -2ik\left(r_1 z_0 + r_2 z_1 + r_5 z_2\right)(F + iG) + r_1(P + iQ) \tag{A6}$$

$$-\mu_2 k^2 z_2 + \mu_2 \lambda_2^2 z_2 = -2ik\left(r_4 z_0 + r_5 z_1 + r_6 z_2\right)(F + iG) + r_4(P + iQ) \tag{A7}$$

$$K_j = \frac{8M_{m_0}}{a\rho c_0 M_{c_0}} k^2\left(z_0 + \frac{M_{m_1}}{M_{m_0}} z_1 + \frac{M_{m_2}}{M_{m_0}} z_2\right) -$$

$$2ik(F + iG)\left(z_0 + \frac{M_{c_1}}{M_{c_0}} z_1 + \frac{M_{c_2}}{M_{c_0}} z_2\right) + (P + iQ) \tag{A8}$$

where $F(k)$ and $G(k)$ are the in-phase and out-of-phase oscillatory lift coefficients and $P(k)$ and $Q(k)$ are the similar in-phase and out-of-phase lift components on a rigid wing subjected to a sinusoidal gust. In equation (A8), K_j represents the bending-moment transfer function $T(f)$ per unit gust velocity at station y_j. By solving equations (A5), (A6), and (A7) simultaneously for values of z_0, z_1, and z_2 and substituting these values into equation (A8), values of K_j may be obtained for any frequency k.

For the present analysis, the bending-moment factor K_j was expressed as strain by use of the following relation:

$$\epsilon = \frac{M_j l}{EI} = \frac{l}{EI}\frac{a}{2}\rho U V M_{c_0} K_j \tag{A9}$$

The airplane loading, physical constants, and basic parameters used in this analysis are listed for each wing station in table I.

REFERENCES

1. Houbolt, John C., and Kordes, Eldon E.: Structural Response to Discrete and Continuous Gusts of an Airplane Having Wing-Bending Flexibility and a Correlation of Calculated and Flight Results. NACA Rep. 1181, 1954. (Supersedes NACA TN 3006; also contains essential material from TN 2763 and TN 2897.)

2. Houbolt, John C., and Kordes, Eldon E.: Gust-Response Analysis of an Airplane Including Wing Bending Flexibility. NACA TN 2763, 1952.

3. Houbolt, John C.: A Recurrence Matrix Solution for the Dynamic Response of Aircraft in Gusts. NACA Rep. 1010, 1951. (Supersedes NACA TN 2060.)

4. Bisplinghoff, R. L., Isakson, G., Pian, T. H. H., Flomenhoft, H. I., and O'Brien, T. F.: An Investigation of Stresses in Aircraft Structures Under Dynamic Loading. Contract No. NOa(s) 8790, M.I.T. Rep., Bur. Aero., Jan. 21, 1949.

5. Goland, M., Luke, Y. L., and Kahn, E. A.: Prediction of Wing Loads Due to Gusts Including Aero-Elastic Effects. Part I - Formulation of the Method. AF TR No. 5706, Air Materiel Command, U. S. Air Force, July 21, 1947.

6. Bisplinghoff, R. L., Isakson, G., and O'Brien, T. F.: Report on Gust Loads on Rigid and Elastic Airplanes. Contract No. NOa(s) 8790, M.I.T. Rep., Bur. Aero., Aug. 15, 1949.

7. Shufflebarger, C. C., and Mickleboro, Harry C.: Flight Investigation of the Effect of Transient Wing Response on Measured Accelerations of a Modern Transport Airplane in Rough Air. NACA TN 2150, 1950.

8. Mickleboro, Harry C., and Shufflebarger, C. C.: Flight Investigation of the Effect of Transient Wing Response on Wing Strains of a Twin-Engine Transport Airplane in Rough Air. NACA TN 2424, 1951.

9. Mickleboro, Harry C., Fahrer, Richard B., and Shufflebarger, C. C.: Flight Investigation of Transient Wing Response on a Four-Engine Bomber Airplane in Rough Air With Respect to Center-of-Gravity Accelerations. NACA TN 2780, 1952.

10. Murrow, Harold N., and Payne, Chester B.: Flight Investigation of the Effect of Transient Wing Response on Wing Strains of a Four-Engine Bomber Airplane in Rough Air. NACA TN 2951, 1953.

11. Press, Harry, and Houbolt, John C.: Some Applications of Generalized Harmonic Analysis to Gust Loads on Airplanes. Jour. Aero. Sci., vol. 22, no. 1, Jan. 1955, pp. 17-26, 60.

12. Press, Harry, and Tukey, John W.: Power Spectral Methods of Analysis and Their Application to Problems in Airplane Dynamics. Vol. IV of AGARD Flight Test Manual, Pt. IV C, Enoch J. Durbin, ed., North Atlantic Treaty Organization, June 1956, pp. IVC:1-IVC:41.

13. Press, Harry, and Meadows, May T.: A Reevaluation of Gust-Load Statistics for Applications in Spectral Calculations. NACA TN 3540, 1955.

TABLE I

AIRPLANE LOADING, PHYSICAL CONSTANTS, AND BASIC PARAMETERS

(a) Terms that apply to all wing stations

W, lb	105,900
V, mph	250
S, sq ft	1,739
b, in.	1,700
Aspect ratio	11.6
Mean aerodynamic chord, ft	12.9
Center-of-gravity position (approximate), percent mean aerodynamic chord	22
a	5.00
c_0, in.	205
ρ, slugs/cu ft	0.00238
ω_1, radians/sec	15.6
ω_2, radians/sec	40.8
μ_0	74.4
μ_1	1.422
μ_2	0.181
λ_1	0.362
λ_2	0.953
r_1	0.190
r_2	0.131
r_4	0.082
r_5	0.068
r_6	0.054

(b) Terms that apply to specific wing stations

Wing station, in.	$\frac{M_{m_0}}{M_{c_0}}$	$\frac{M_{m_1}}{M_{m_0}}$	$\frac{M_{m_2}}{M_{m_0}}$	$\frac{M_{c_1}}{M_{c_0}}$	$\frac{M_{c_2}}{M_{c_0}}$	l, in.
126	0.834	0.154	-0.015	0.455	0.205	16.9
255	.562	.230	-.0015	.536	.262	15.3
432	.155	.496	.179	.661	.388	13.1
590	.089	.700	.452	.786	.571	11.3

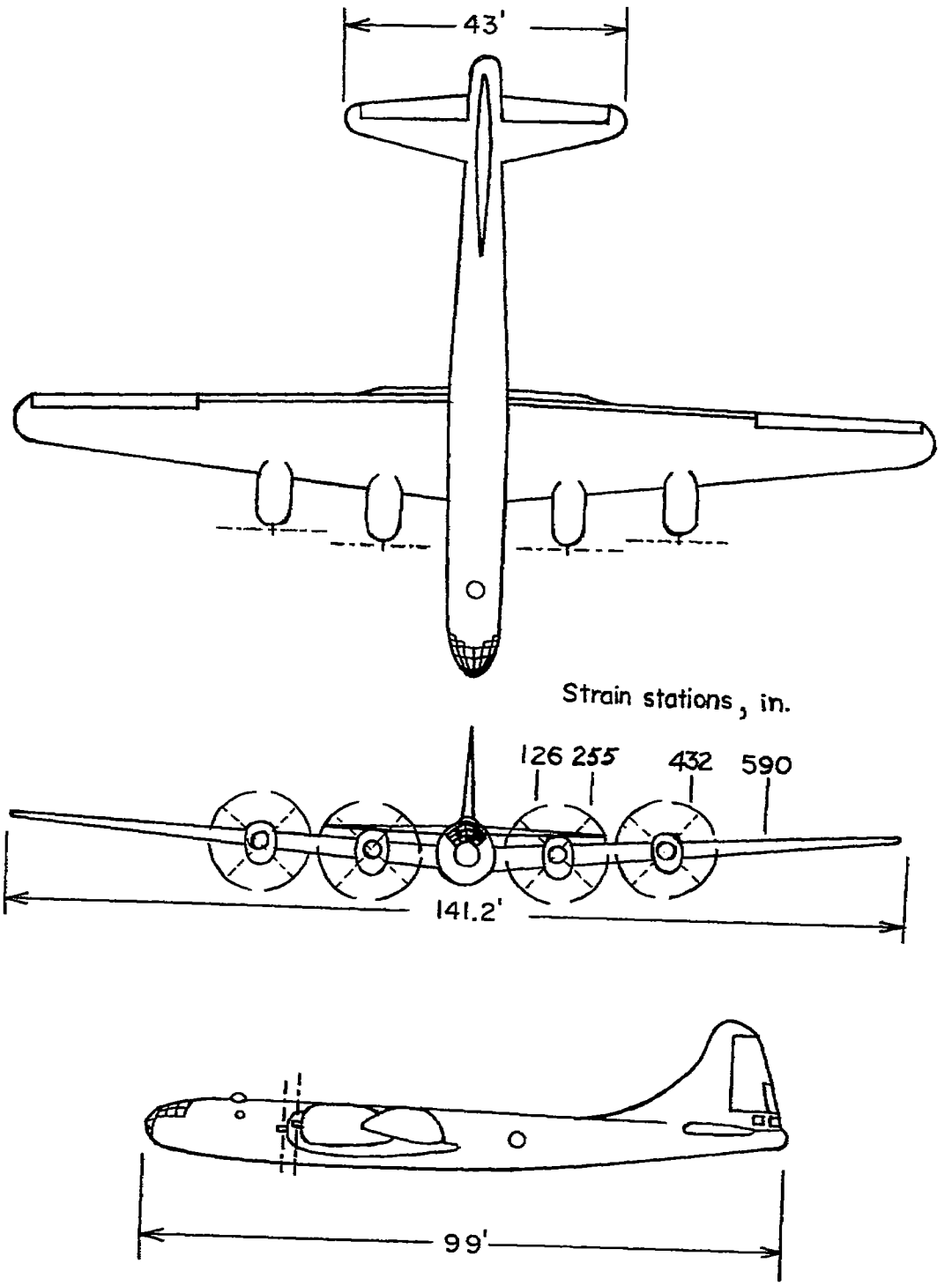

Figure 1.- Three-view drawing of test airplane.

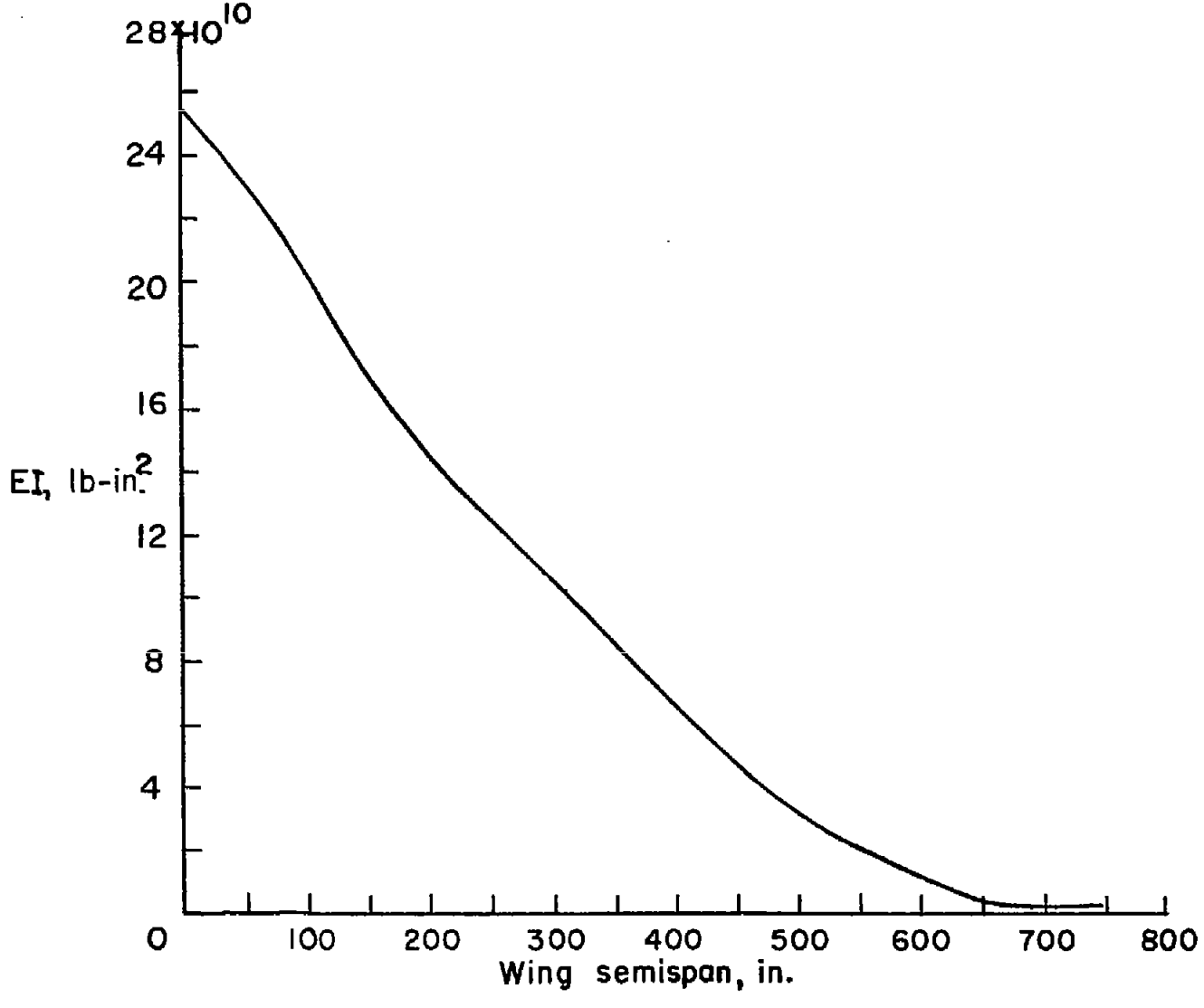

Figure 2.- Estimated spanwise stiffness distribution.

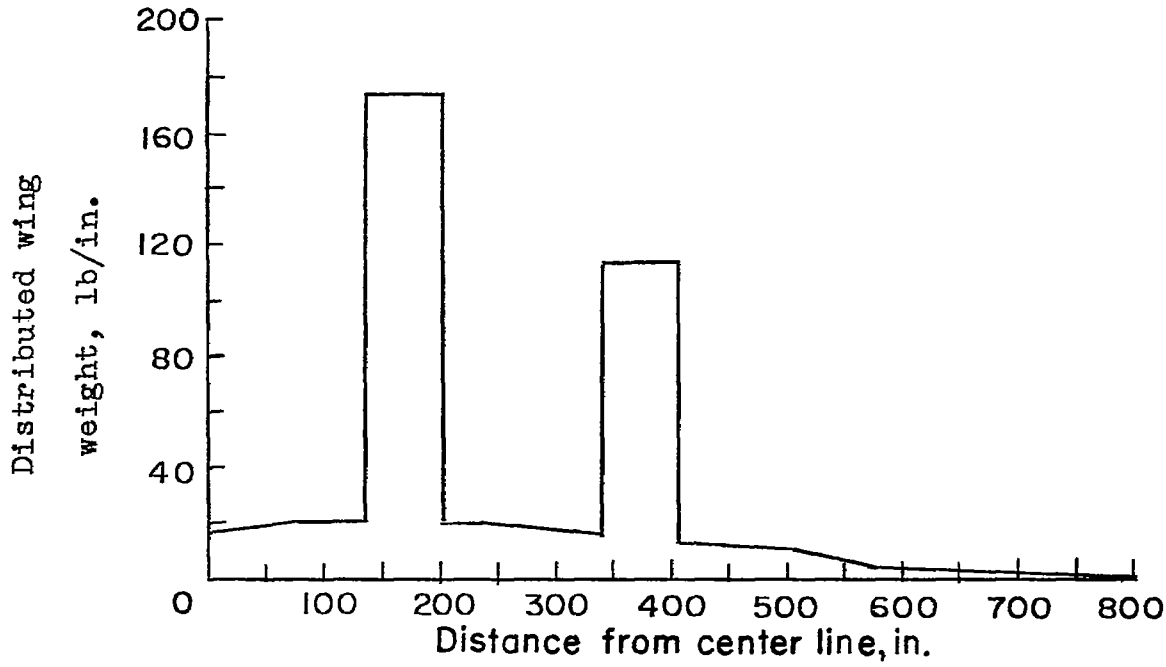

(a) Wing structure and nacelles.

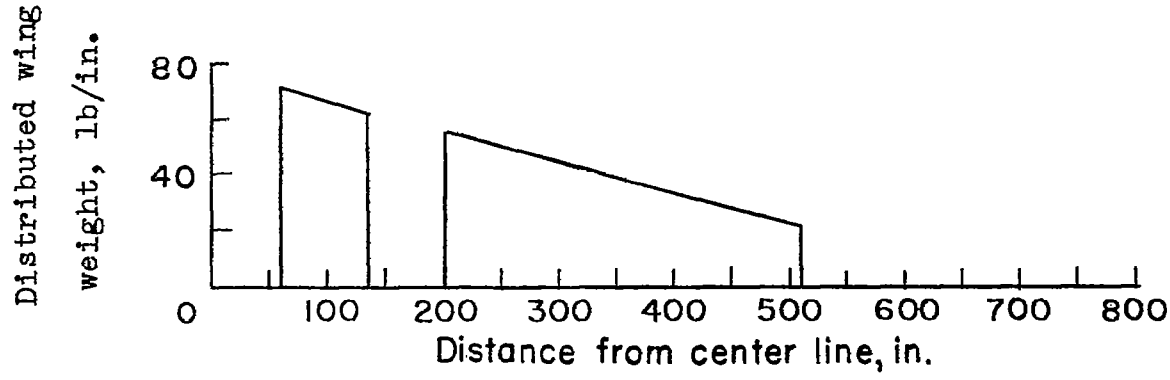

(b) Fuel load.

Figure 3.- Estimated spanwise weight distribution for a gross weight of 105,900 pounds.

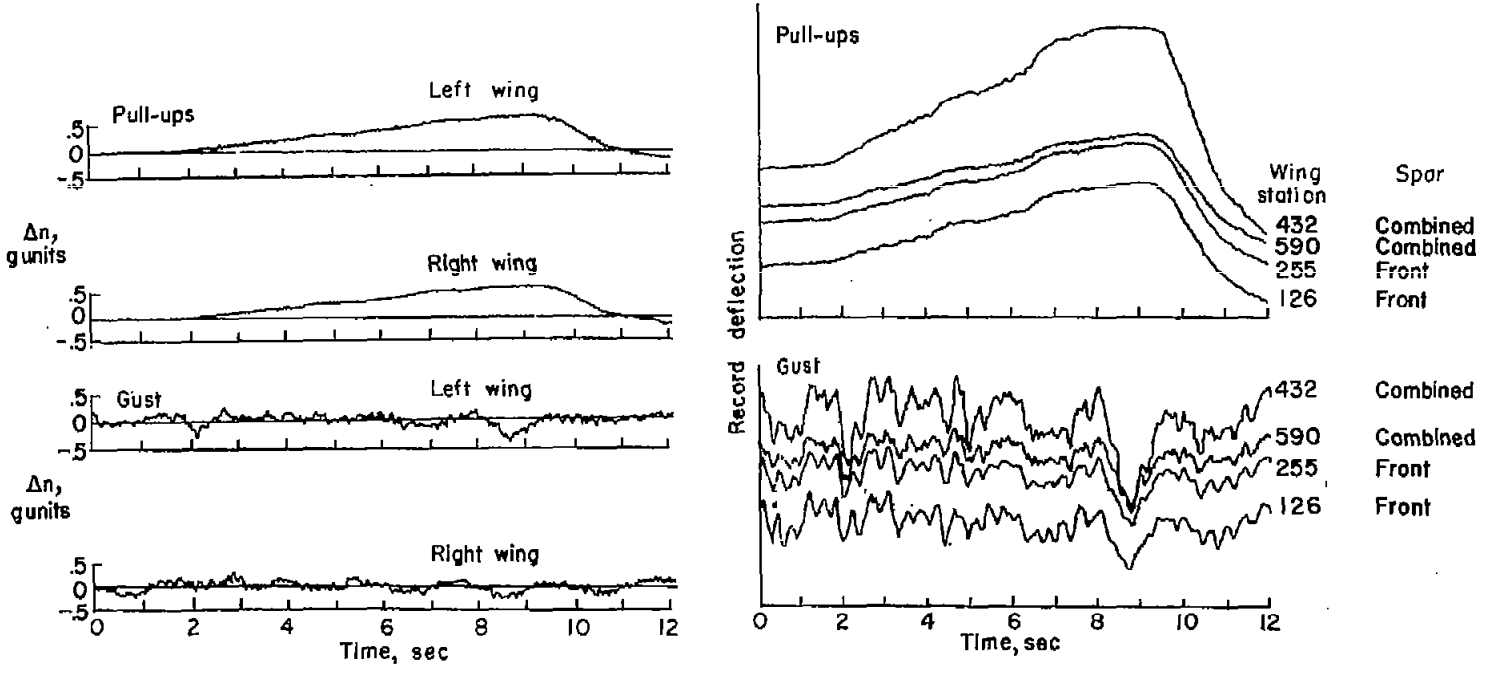

(a) Nodal accelerations.

(b) Wing-strain indications.

Figure 4.- Time histories of nodal accelerations and wing-strain indications.

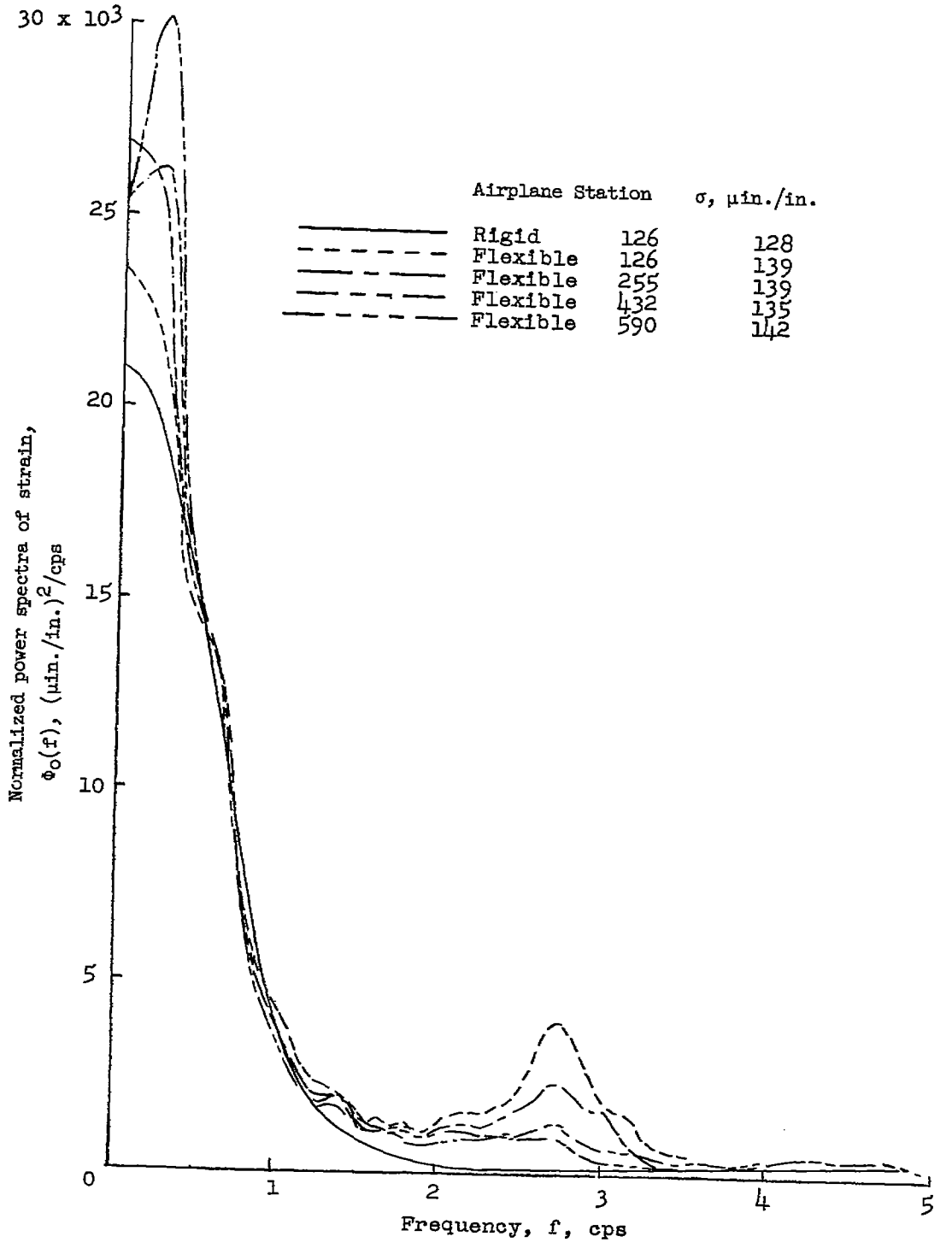

Figure 5.- Measured strain spectra (normalized to strain at station 126).

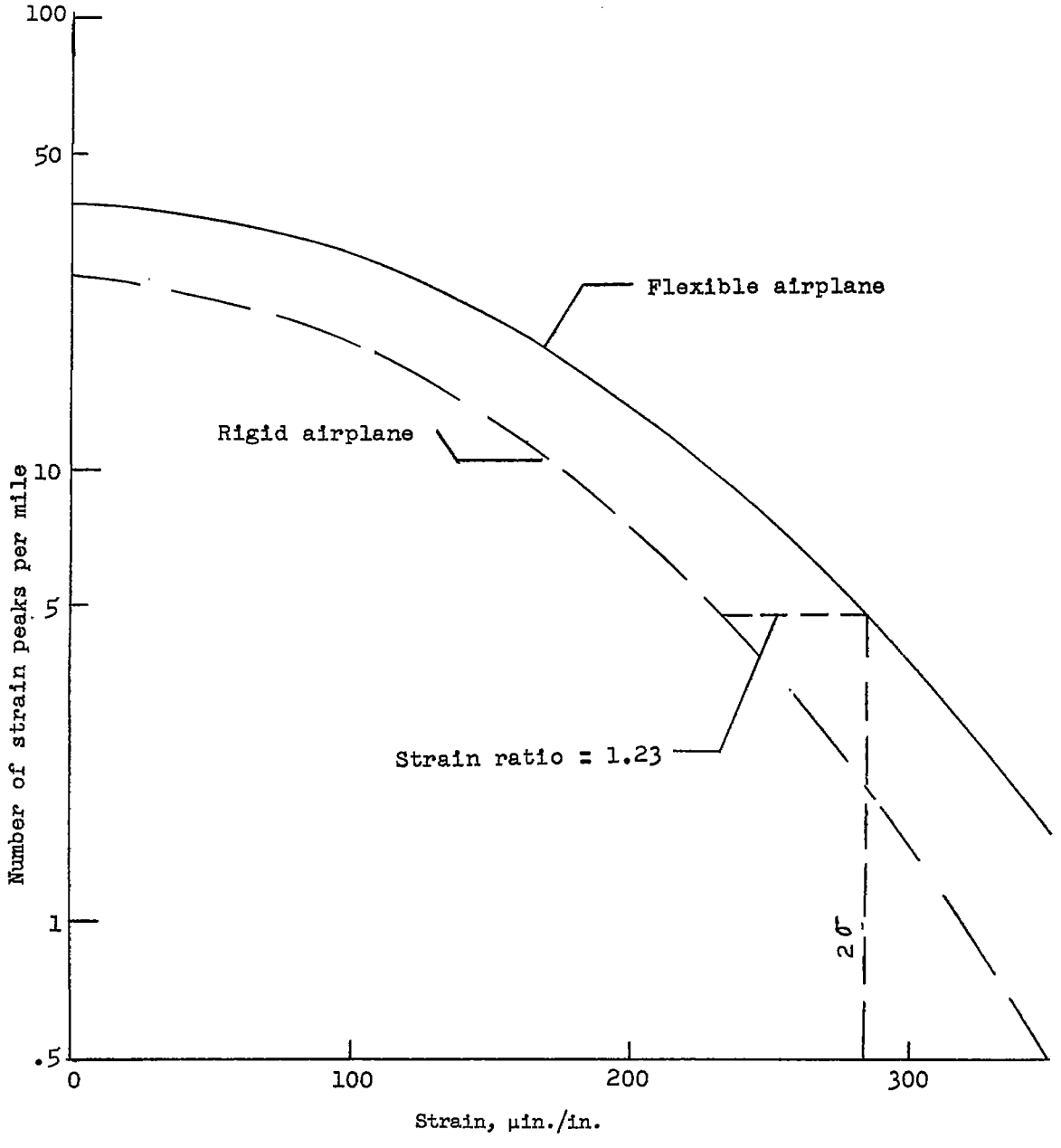

Figure 6.- Variation of the number of strain peaks with strain level for the rigid and flexible conditions at station 126 (estimated from measured spectra and eq. (3)).

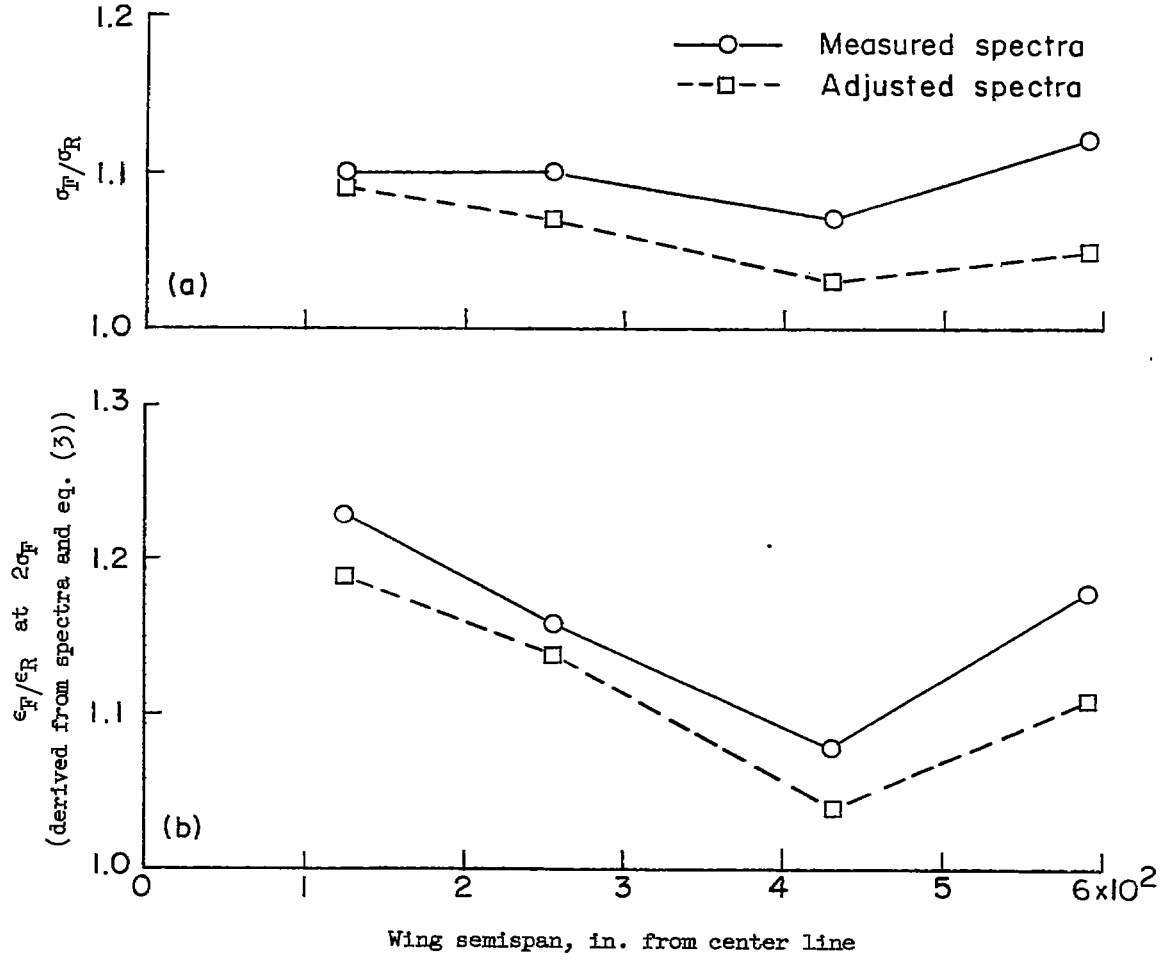

Figure 7.- Measured strain amplification factors.

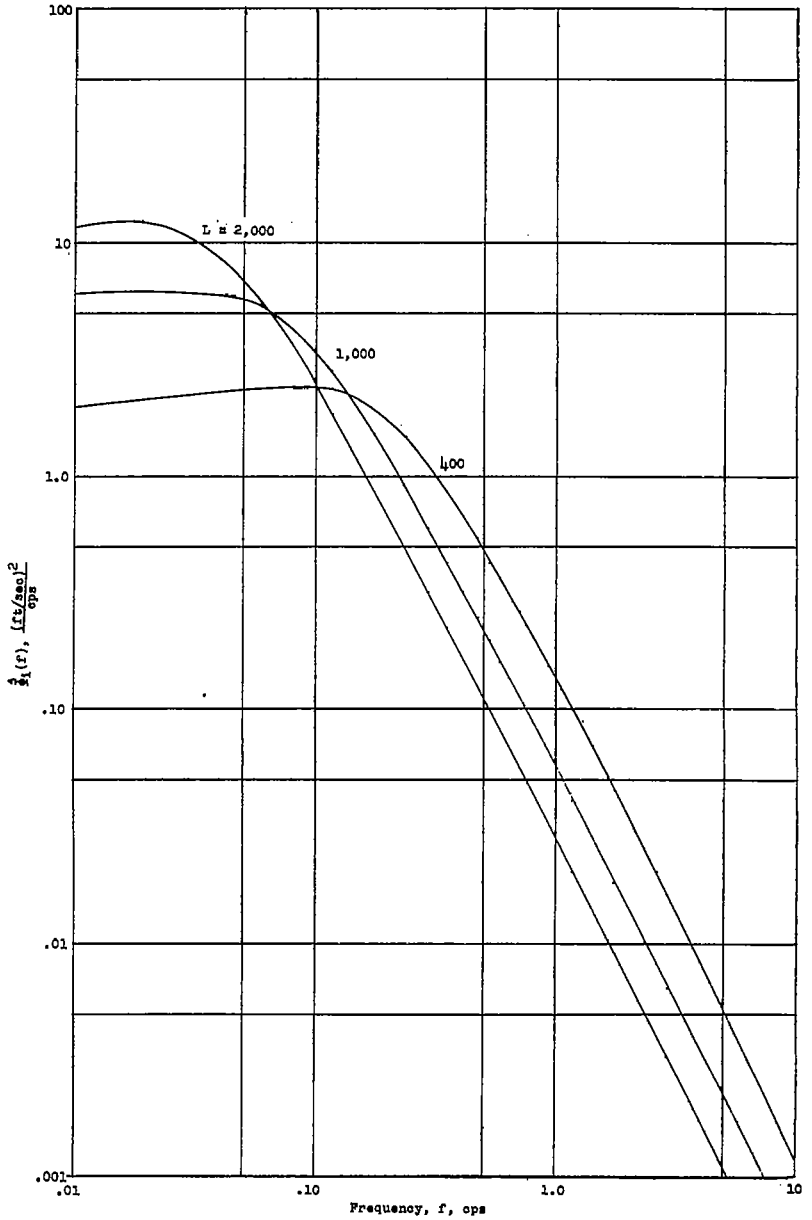

Figure 8.- Assumed gust input spectrum.

$$\hat{\Phi}_i(f) = \sigma_U^2 \frac{2L}{V} \frac{1 + 3\left(\frac{2\pi Lf}{V}\right)^2}{\left[1 + \left(\frac{2\pi Lf}{V}\right)^2\right]^2}; \quad \sigma_U^2 = 1.$$

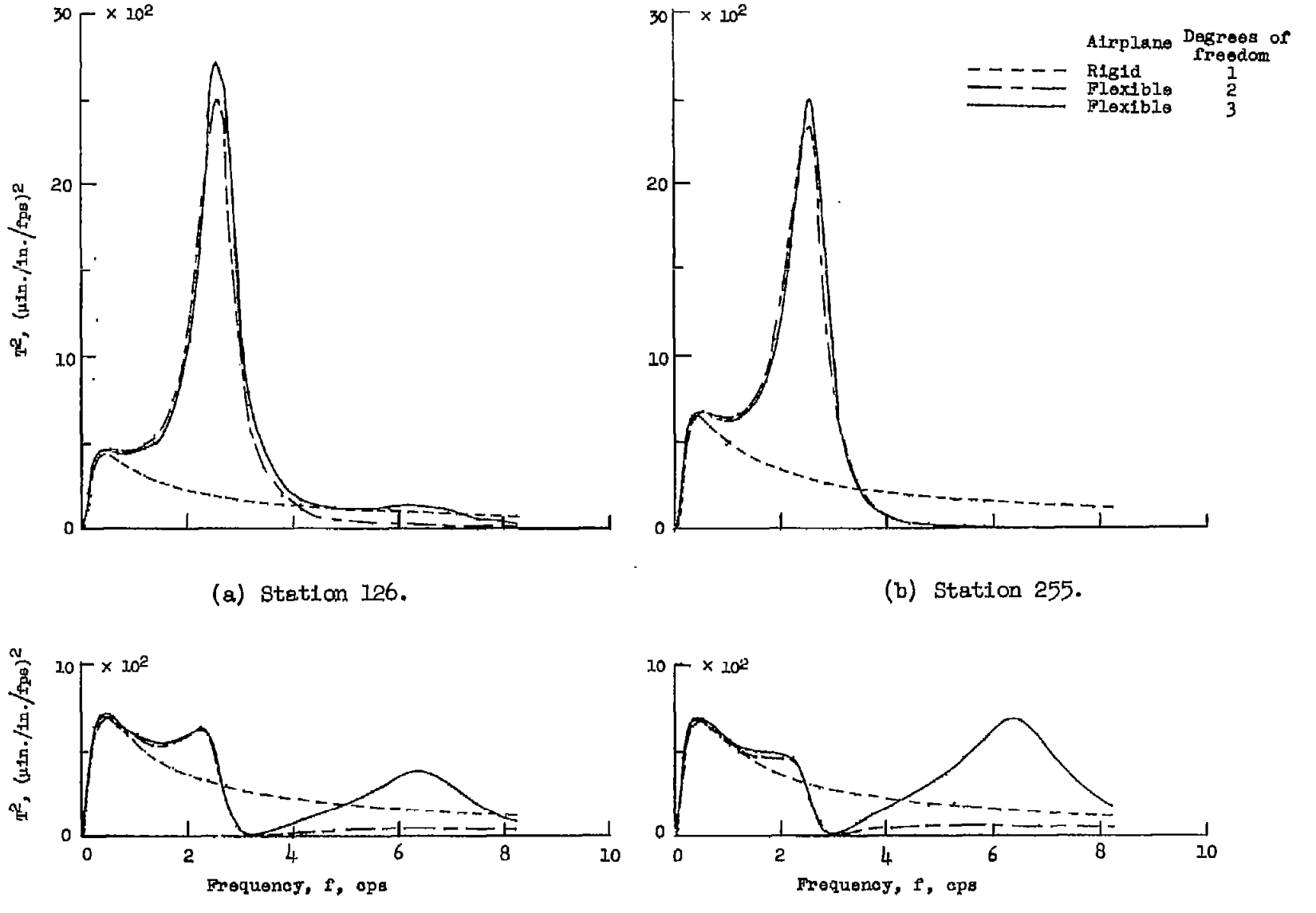

(a) Station 126.

(b) Station 255.

(c) Station 432.

(d) Station 590.

Figure 9.- Theoretical transfer functions. a = 5.00.

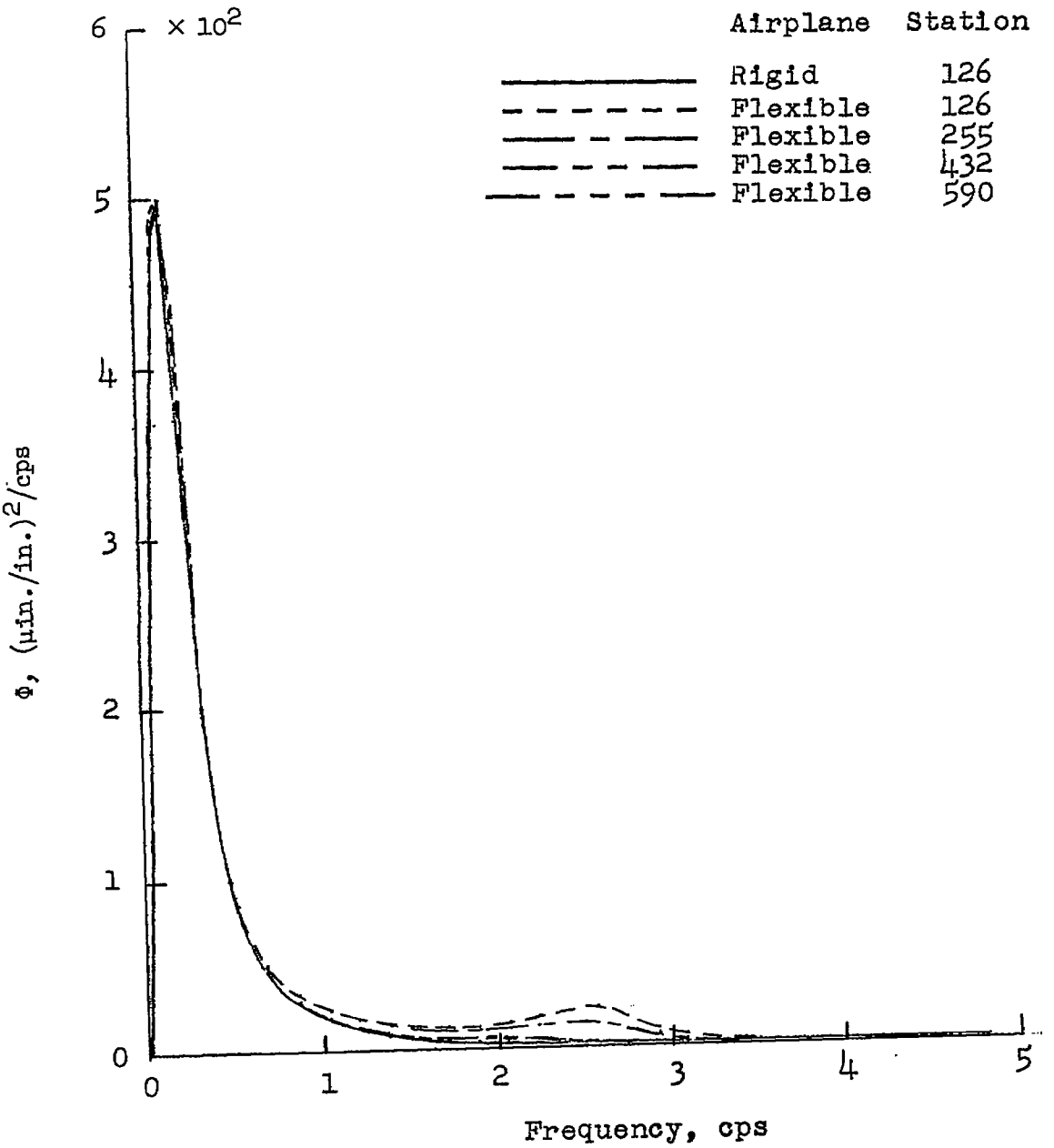

Figure 10.- Power spectra of strain at four wing stations normalized to strain at station 126. L = 1,000 feet.

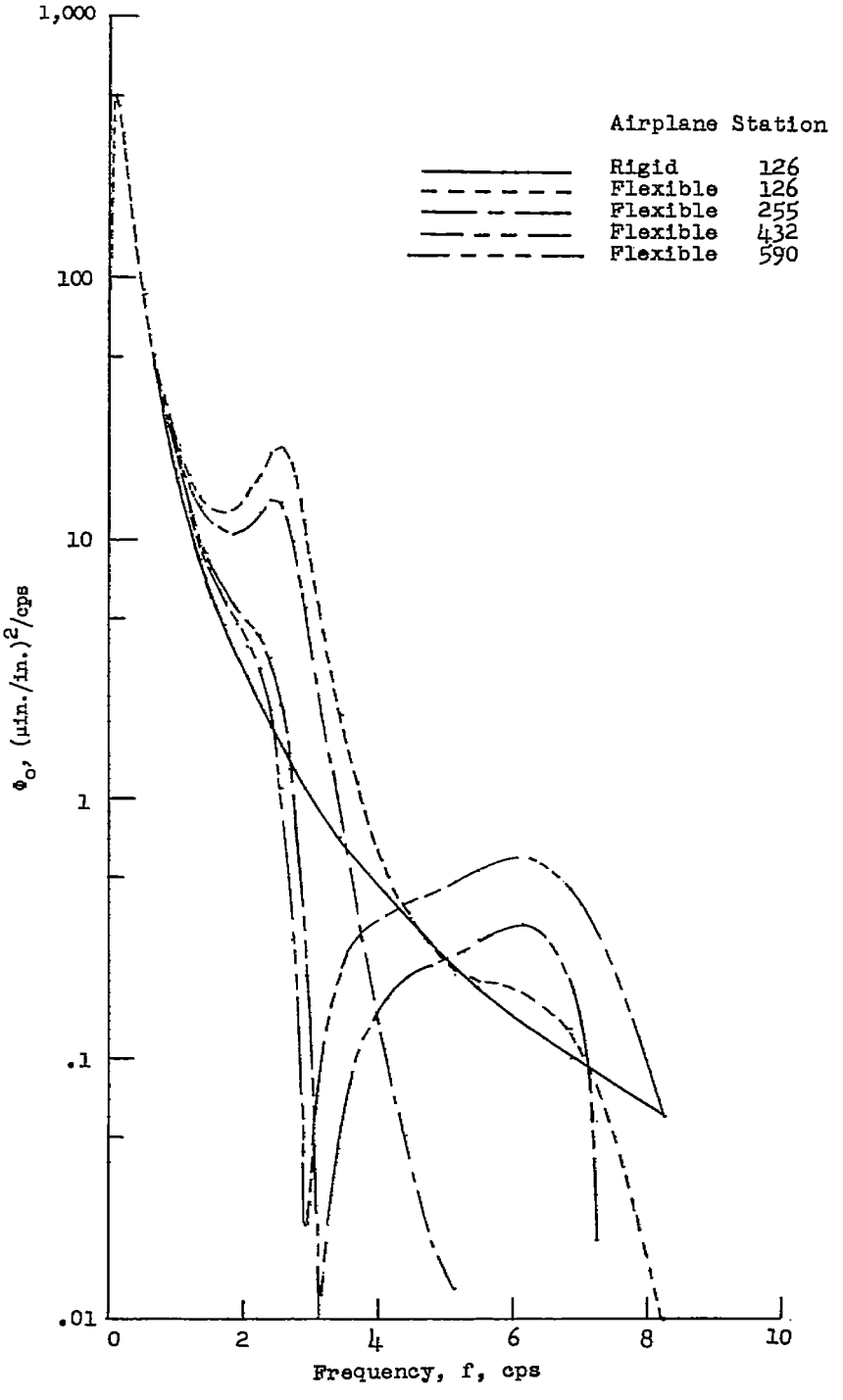

Figure 11.- Power spectra of strain to 10 cps at four wing stations normalized to strain at station 126. L = 1,000 feet.

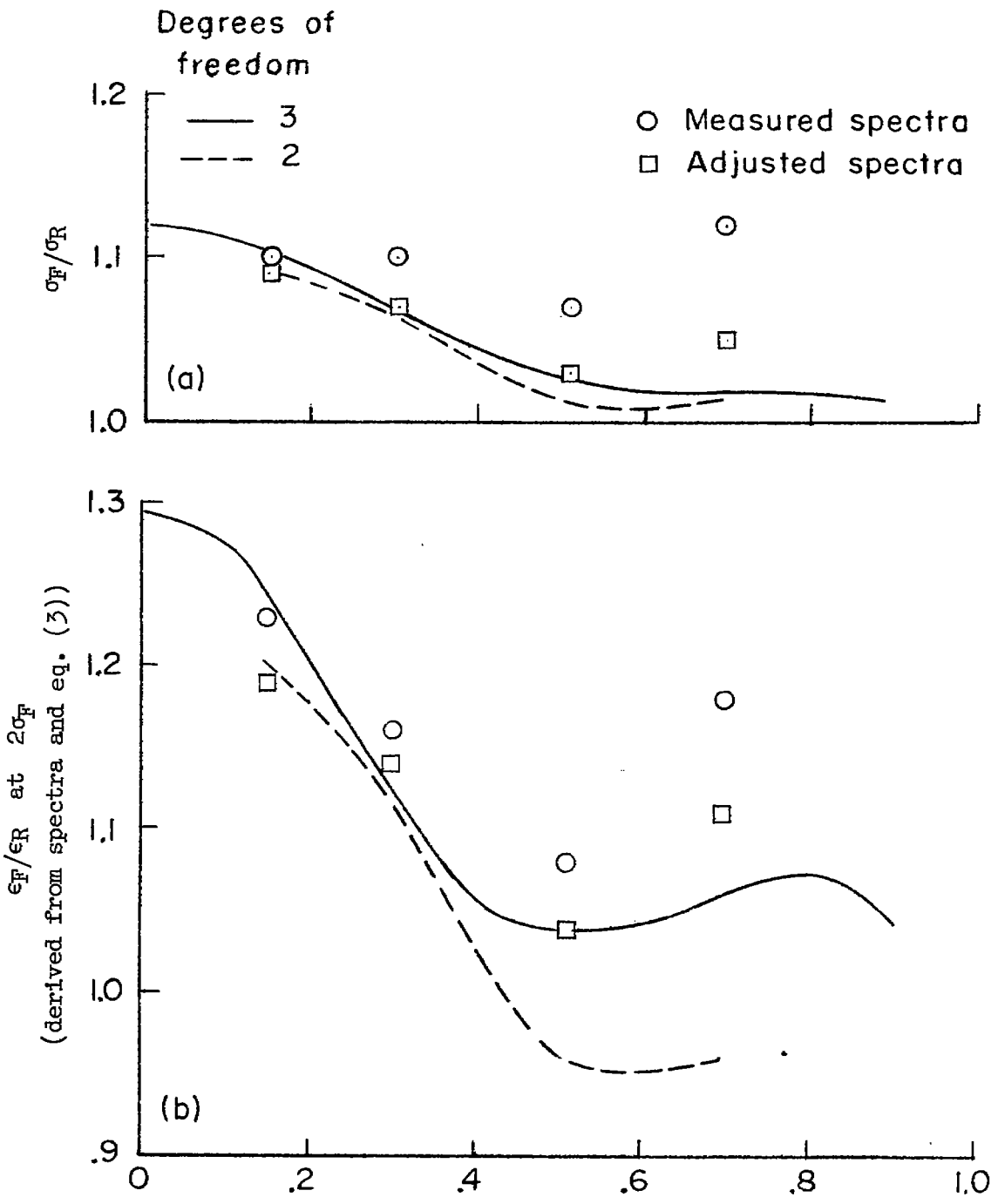

Figure 12.- Calculated and measured strain and amplification factors. L = 1,000 feet.